HIGH REYNOLDS NUMBER SIMULATION IN A TRANSONIC WIND TUNNEL BY SURFACE SUCTION

John E. Green, Mike Elliott, Peter W. C. Wong
Aircraft Research Association Ltd, Manton Lane, Bedford MK41 7PF, UK

Keywords: *wind tunnel tests, high Reynolds number, scale effect, porous boundary layer control.*

Abstract

The paper reports a theoretical and experimental investigation, the objective of which was to demonstrate the feasibility of simulating the aerodynamics of a transport aircraft wing at full scale Reynolds numbers by applying boundary layer suction to a semi-span model tested at atmospheric stagnation pressure in the ARA 9ft by 8ft Transonic Wind Tunnel (TWT). The programme was wide ranging, multi-disciplined, complex and difficult. It required new ground to be broken on a number of fronts before the final goal was reached. With one exception, the intermediate objectives were achieved, as was the main goal of demonstrating the potential of boundary layer suction as a means of simulating higher Reynolds numbers. The paper outlines the research programme and presents the salient results. Comparisons between results on a swept-winged semi-span model, tested with suction in the ARA TWT, and data from a full-span model of the same geometry, tested under cryogenic conditions in ETW, demonstrate the feasibility of this form of simulation.

Nomenclature

A	Aspect ratio, empirical constant
c	Aerofoil chord
C_D	Drag coefficient
C_{D0}	Drag coefficient adjusted for lift and suction
C_{D0W}	C_{D0} for wing alone
C_L	Lift coefficient
C_m	Pitching-moment coefficient
C_{mc}	Pitching-moment coefficient at "break" in curve
C_p	Pressure coefficient
C_{qt}	Total suction coefficient over a panel, surface or wing
C_{qu}, C_{ql}	Values of C_{qt} for upper and lower surfaces respectively
C_x	Generalised force or moment coefficient
k	Weighting parameter for lower surface suction
m_s	Total suction mass flow
M	Mach number
p	Static pressure
R	Reynolds number
S	Gross wing area
U_∞	Free stream velocity
v_w	Suction velocity
x	streamwise distance in Cartesian co-ordinates
x_t	Value of x at boundary-layer transition
α	Angle of incidence
δ^*	Boundary-layer displacement thickness
θ	Boundary-layer momentum thickness
ρ_∞	Density in free stream
ρ_w	Density at wall

1 Introduction

This paper describes a theoretical and experimental investigation of the application of boundary layer suction to a model of a transport aircraft in the ARA Transonic Wind Tunnel (TWT), tested at atmospheric stagnation conditions, as a means of simulating aerodynamic behaviour at full scale Reynolds numbers. The programme was wide-ranging and technically challenging, requiring advances on several fronts into more or less unknown territory. It was funded jointly by DTI, BAe (now Airbus UK) and ARA and was designated

R20. In this paper it will be possible to present only the salient results.

The principle reason for undertaking the R20 programme was the potential economic benefit to be gained by designing civil aircraft wings to take full advantage of the higher aerodynamic performance achievable at full scale Reynolds numbers. Historically, designs in the UK could only be demonstrated at the maximum Reynolds number available in a UK wind tunnel (6 million, in the recently closed 8ft x 8ft wind tunnel at QinetiQ, Bedford). It has long been known [1] that performance gains are achieved by designing at flight Reynolds number, but such designs had to take into account that they would have to be demonstrated/validated at relatively low Reynolds numbers and using current methodology to then scale from wind-tunnel to flight conditions.

With the advent of the European Transonic Wind Tunnel (ETW), however, the prospect opened up of validating transport aircraft with wings designed to for optimum performance at flight Reynolds number. The programme reported here was conceived primarily as a back-up to ETW, to reduce the risk entailed in the European industry committing to a design philosophy which depended critically on a single wind tunnel facility for design validation at flight Reynolds numbers. The technique investigated, if successful, would enable tunnels such as the ARA TWT to support testing in ETW, either for specialised tests (such as powered propulsion testing) not yet available in ETW or, in the event of any major outage of ETW, as an alternative facility for more general testing.

The proposed use of boundary layer suction in the wind tunnel is essentially an extension of the well established and well understood technique of aft transition fixing that is in general use in transonic testing at ARA and elsewhere. Its potential was demonstrated by theoretical modelling, on the basis of which a strong case was made for a full-blown experimental test of its feasibility. There were however, some important aspects of boundary layer behaviour which were not well understood and which had an important bearing on the application of the technique. The total programme therefore consisted of a series of basic experimental and theoretical studies aimed at creating a foundation on which the main test programme, on a swept-winged semi-span model in the TWT, could be built. From the results of this test programme, it appears that the programme has achieved its principal aim. Boundary layer suction appears to be a powerful, flexible and credible means of simulating high Reynolds numbers and the programme has enabled a practicable methodology for its application to be developed.

2 High R Simulation

2.1 Scale effects and full scale extrapolation

The concept of Reynolds number, as aerodynamic scale, was first proposed by Lanchester in 1907, [2]. The underlying principle is that true aerodynamic equivalence is achieved only if geometry and Reynolds number (and, in compressible flow, also Mach number) are identical. Fortunately, aerodynamic behaviour varies only slowly with Reynolds number. As a result, early workers found that useful aerodynamic data could be obtained from wind tunnel tests on scale models, at Reynolds numbers much lower than flight, provided that the boundary layer over the key surfaces of the wind tunnel model was in the same state - laminar or turbulent - as in flight. The use of transition trips - roughness elements which promote premature transition of the boundary layer from laminar to turbulent - became normal wind tunnel practice. By the 1960s, transition fixing was a well developed and well understood technique, at least as far as the required properties of the roughness elements were concerned.

In the mid 1960s, however, confidence in wind tunnel tests at transonic conditions was undermined by the large differences between wind tunnel and flight that were found for the Lockheed C 141 military transport aircraft. There were several other examples from around that time of important discrepancies between wind tunnel and flight and collectively, with the C 141 as the most cited example, they became the core of the case for building transonic wind tunnels that can reproduce full scale Reynolds numbers. As a result, the National Transonic Facility (NTF) was built at NASA Langley and the ETW at Cologne.

As early as 1966, however, Loving [3] showed for the C 141 that it was possible to obtain wind tunnel results much closer to those in flight by adopting a more aft position for the transition trip on the model wing. Loving considered the most important factor in the C 141 wing aerodynamics to be the onset of boundary layer separation at the trailing edge. He showed, by boundary layer calculations, that the use of an aft trip in the wind tunnel should enable similar values of the boundary layer shape parameter H at the trailing edge, and hence similar margins from separation, to be obtained in wind tunnel and flight. The new wind tunnel results supported this idea.

2.2 Simulation of full scale

The way in which the boundary layer and the external flow interact, and hence the way in which boundary layer development influences overall aerodynamic behaviour, was discussed in [4], where the idea of using boundary layer suction to simulate higher Reynolds number was also proposed and explored theoretically. The proposal to use suction was repeated, with further explanation, in [5]. Meanwhile, over the years since Loving demonstrated its effectiveness, the aft transition trip has established itself as a useful though limited tool for simulating higher Reynolds numbers. Other, more general techniques for extrapolating from wind tunnel to flight have become quite sophisticated and AGARD has published recommendations [6] on how to minimise errors in extrapolation from tests at Reynolds numbers an order of magnitude lower than full scale. The recommendations are complex and have probably been implemented in full only rarely, if at all.

The aim of the present programme is to demonstrate a technique which enables full scale aerodynamic behaviour to be *simulated* at the Reynolds numbers of the ARA Transonic Wind Tunnel, thereby avoiding the need to extrapolate. The key premise is that correct simulation of boundary layer displacement thickness will result in correct simulation of pressure distribution and hence of overall aerodynamics. Determining the extent to which, if this is achieved for the cruise condition, other features (drag, buffet margin) are also simulated was one aim of the investigation.

In [4] it was shown that, if the current theoretical models of turbulent boundary layer structure are reliable, an appropriate distribution of suction over the entire wing surface should enable boundary layer behaviour at a higher Reynolds number to be simulated precisely over virtually the whole of the wing. From an engineering standpoint, this is not practicable and a compromise must be made between fidelity of simulation and engineering complexity.

In this context, the three most important regions of boundary layer development are: over the rear upper surface of the wing; over the rear lower surface; and in the region of interaction with the shock wave on the upper surface. During the course of the programme, an understanding of what compromises would be needed in the main experiment with the semi-span model in the TWT, in order to achieve a good simulation of the boundary layer in these three regions, emerged only slowly. The method finally adopted for the semi-span model used a

combination of aft transition fixing and boundary layer suction over the rear of the upper and lower wing surfaces.

3 Scope of the R20 Programme

The total programme was planned to include a number of basic experiments on boundary layer skin friction in low speed flow, experiments on pressure loss in suction ducts, development of a range of theoretical treatments of both the internal and external flows and tests on a two-dimensional aerofoil with suction, all as a preliminary to the final tests on a swept-winged semi-span model in the TWT. In parallel with this, techniques were developed for the design and manufacture of wind tunnel models with boundary layer suction, together with the plant needed to remove the suction flow from the model without compromising force and moment measurements. Finally, prior to the tests in the TWT, a methodology for simulating a specific target "full scale" Reynolds number had to be devised.

The programme encountered some difficulties. Not all of the planned basic experimental work was completed, not all the theoretical modelling showed good agreement with experiment and the development of techniques for manufacturing wind-tunnel models with laser-drilled suction surface presented a number of challenges and lessons for the future. This paper concentrates on the two key high-speed wind tunnel tests, in the ARA 2D Tunnel and the TWT, the support of these tests by the aerofoil viscous analysis code BVGK [7], and the positive inferences we draw from the tests.

4 Studies in Two Dimensions

4.1 Parametric investigations using BVGK

As part of the prior studies to build the case for undertaking the programme, the transonic viscous aerofoil program BVGK [7] was modified to include the effect of surface suction on the development of the turbulent boundary layer. The turbulent boundary layer method in BVGK is an extension of the lag-entrainment method [8] with the inclusion of higher order terms and the "inverse" mode of solution. In comparisons with benchmark tests in the DERA 8ft × 8ft tunnel, BVGK has proved to be a highly accurate and reliable code for two-dimensional aerofoils with solid surfaces. In the first implementation of the modified version of the code, the effect of suction on all aspects of the boundary layer and external flow were correctly modelled with the exception of the effect of suction on the skin-friction coefficient. In subsequent work, three alternative models of the effect of suction on skin friction were derived (termed models A, B and C)

The prior studies included illustrative calculations using the earliest version of BVGK with suction. These were done for the RAE 5234 aerofoil at a section Mach number of 0.73 and lift coefficient of 0.77, a typical cruise condition for a long-range transport aircraft.

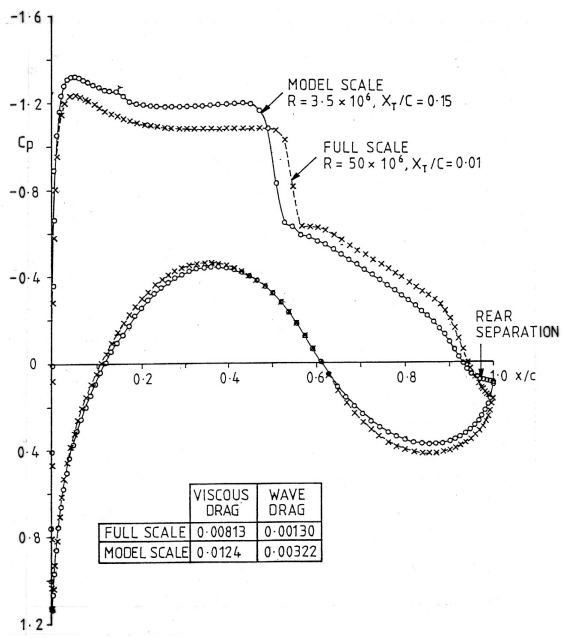

Figure 1. Differences in the pressure distributions and drag between full and model scale Reynolds numbers for RAE 5234 aerofoil, M = 0.73, C_L = 0.77

Fig 1 shows the calculated pressure distributions over a solid aerofoil at chord Reynolds numbers of 3.5 and 50 million, characteristic respectively of a model in the ARA TWT and an aircraft in flight. The viscous and wave drag coefficients for the two cases are shown inset. The differences in pressure distribution and drag are substantial. Fig 2 shows the calculated effect of applying boundary layer suction over 30% of the upper and lower aerofoil surfaces (the heavily lined areas) at the lower Reynolds number. The pressure distributions at 3.5 and 50 million are now very similar and the calculated drag components are also in better agreement.

Figs 3 and 4 compare the streamwise distributions of boundary layer displacement thickness on the upper and lower surfaces of the aerofoil for the three calculated cases. The effect of suction at 3.5 million is to reduce the displacement thickness over the rear of both surfaces by almost 50%, so that, on both surfaces, the thickness distribution in the trailing-edge region is close to that without

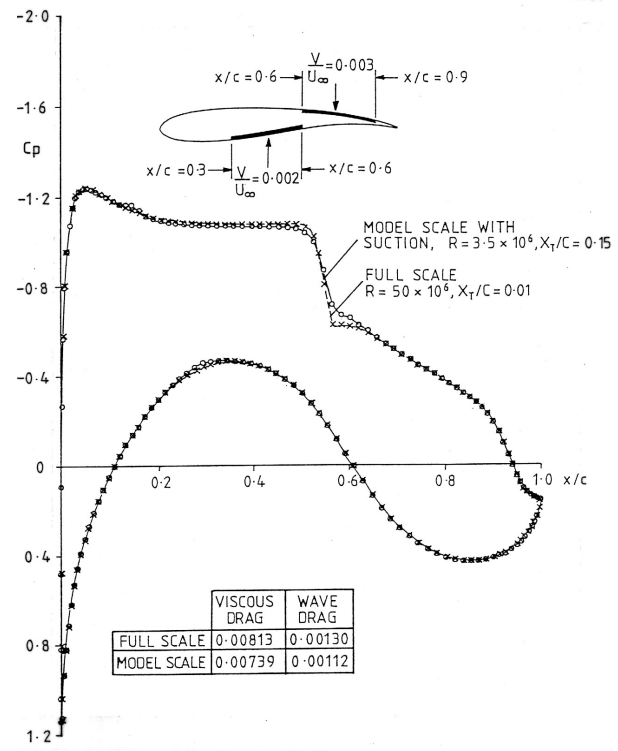

Figure 2. Simulation of full scale Reynolds number for RAE 5234 aerofoil using suction, M = 0.73, C_L=0.77 (unmodified skin-friction formula)

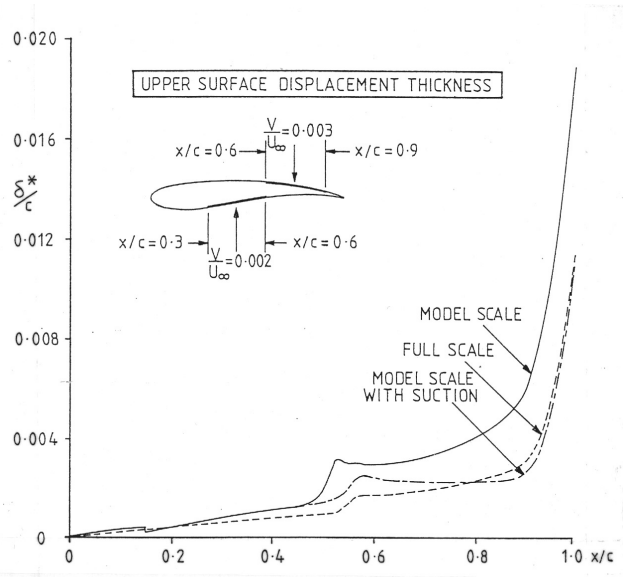

Figure 3. Simulation of full scale Reynolds number for RAE 5234 aerofoil using suction, M = 0.73, C_L=0.77 (unmodified skin-friction formula)

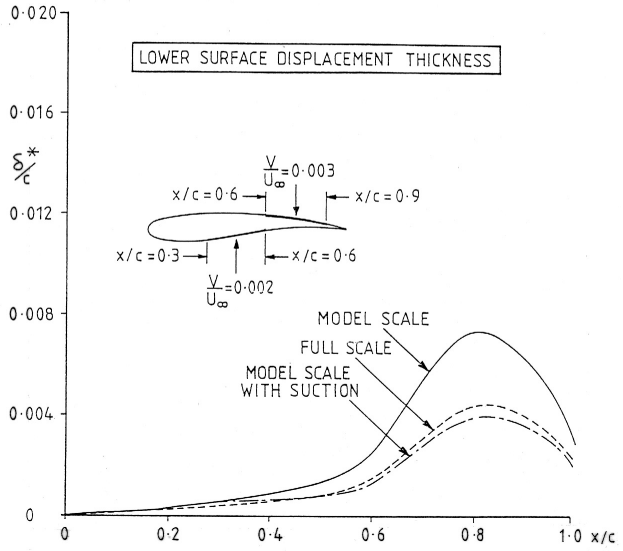

Figure 4. Simulation of full scale Reynolds number for RAE 5234 aerofoil using suction, M = 0.73, C_L=0.77 (unmodified skin-friction formula)

suction at 50 million. It should be noted that this is a first-order simulation, with no attempt to "fine-tune" the suction rate beyond the first significant figure.

The suction model used for the above calculations, which were done before the beginning of the programme, did not allow for the effect of suction on skin friction. This deficiency was corrected before any BVGK calculations were done within the funded

programme. Broadly speaking, the suction needed to achieve a given change in pressure distribution increased by between 30% and 100%, depending on which of the skin friction models (A, B or C) was adopted. As part of the preparation for the high-speed wind tunnel tests, parametric calculations by BVGK were done, covering a wide range of flow conditions and using all three skin-friction models. The calculations strengthened the belief that suction could provide a good simulation of higher Reynolds numbers but also underlined the importance of understanding the effect of suction on skin friction. In the absence of definitive information on this effect, all planning and design for both the 2DT and TWT tests had to make provision for the uncertainty in the skin friction model.

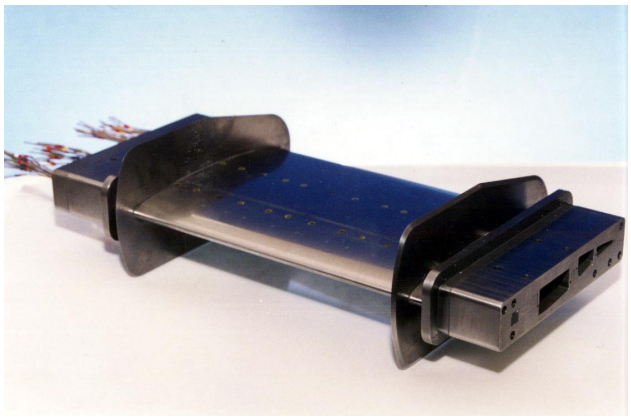

Figure 5. 2D aerofoil: overall view

4.2 Two-dimensional aerofoil tests

The two-dimensional test of an aerofoil with boundary layer suction provided the first practical opportunity to prove the concept of high Reynolds number simulation and to check some of the supporting theory against experiment. The ARA 2D Tunnel used for these experiments has been a source of aerofoil, aircraft and rotor blade sectional data for over 20 years. Its 450mm high by 200mm wide test section allows a model of 127mm chord which, over the tunnel's stagnation pressure range of 1.5 to 4.0 bar, gives a Reynolds number range of 2.7 to 7.5 million at Mach 0.8. The aerofoil section adopted for this part of the programme was RAE 5234. This design was typical of current wings without being commercially sensitive and had been tested over a range of Reynolds numbers in the DERA 8ft × 8ft tunnel.

Fig 5 is a three quarters view of the aerofoil model, showing the detachable boundary- layer fences which it is standard practice to fit to 2D Tunnel models to improve the two-dimensionality of the flow. The model had three sections of perforated wall, two on the upper surface and one on the lower, each with its own suction duct which passed out of the tunnel sidewall through the wing tip. The three ducts, which enabled the suction flow through the three surfaces to be controlled and measured independently, are clearly seen in Fig 5. The model had detailed pressure plotting from which lift and pitching moment were obtained whilst profile drag was derived from a multi-head pitot rake mounted two chord lengths downstream.

The model was designed to allow suction rate to be varied by a factor of at least two by varying the pressure ratio across the perforated surfaces, from approximately 1.1 to 2.0. In order to achieve a uniform suction distribution at the lower pressure ratio, with a typical aerofoil pressure distribution over the suction panels, the porosity of each panel was varied linearly from front to rear by varying the spacing of

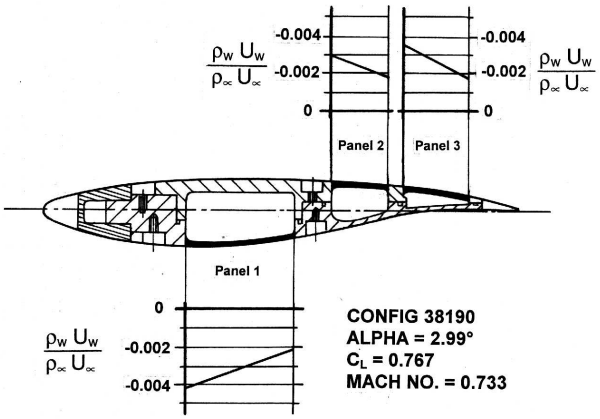

Figure 6. 2D aerofoil:
construction and typical suction distributions

successive lines of holes while keeping the hole size constant. At the higher pressure ratio, suction rate then varied linearly across each panel. This effect is illustrated in Fig 6, which also shows the location of the suction panels and details of the model construction.

On the basis of the BVGK calculations, the suction rates needed to simulate a factor of 10 increase in Reynolds number were determined and porosity distributions specified which would enable this to be achieved. If skin-friction model C proved the more accurate (as was expected) this would be achieved at a pressure ratio of 1.1. If model A proved more accurate, a pressure ratio of 2 would be required. The specified diameter for the suction holes was 0.076mm. In the event, although the laser drilling contractor had consistently achieved target hole sizes in test pieces, the average diameter of the holes in the model panels was 0.057mm. The achieved porosity was thus only 56% of the target value and consequently much of the testing in the 2D Tunnel was done at a pressure ratio in excess of 2, ie at the maximum obtainable suction rate.

The design Mach number of the RAE 5234 aerofoil is 0.73 and most tests were at this Mach number, at a Reynolds number of either 3.5 million or 6.0 million. The position of the ballotini transition strip was varied, as was suction rate, and tests were done with one, two or all three suction ducts in operation. Tests were also done with the perforated panels sealed with gum arabic and rubbed down to restore the original contours.

For transition fixed at 5% chord, fig 7 shows the lift curves with and without suction at a Reynolds number of 6 million. Fig 8 shows corresponding curves without suction at Reynolds numbers of 3.5 million and 6 million. The curves have a characteristic "knee" at an incidence in the region of 2° and, within the

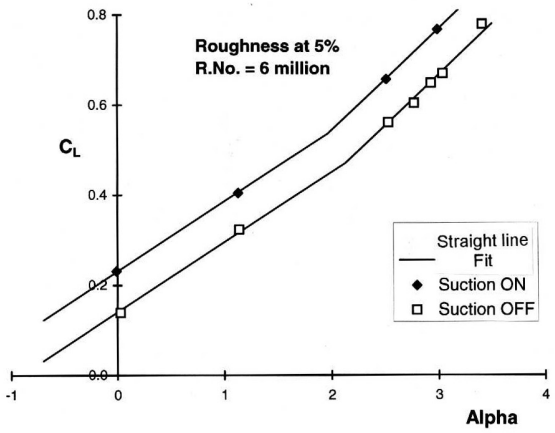

Figure 7. 2D aerofoil: C_L v alpha, M = 0.73 effect of suction

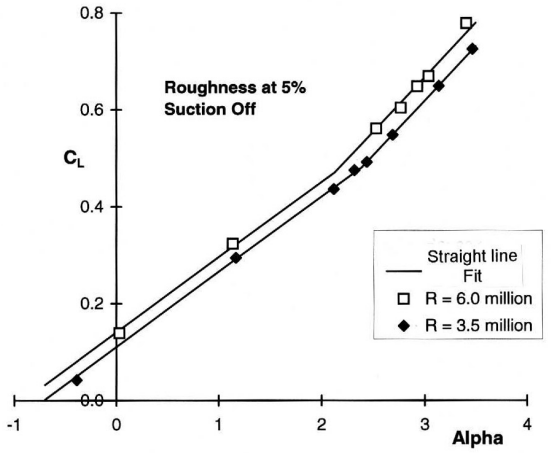

Figure 8. 2D aerofoil: C_L v alpha, M = 0.73 effect of Reynolds number

experimental scatter, are effectively parallel straight lines above and below the knee. As an aid to consistent interpretation of the results, each set of data has been fitted with lines of slope 0.225 per degree and 0.155 per degree passing through the respective centroids of the data points above and below the knee.

The tests show the effect of full suction to be virtually the same at both Reynolds numbers. At a corrected incidence of 2.5° the effect of opening all three suction valves is to increase the corrected lift coefficient by 0.1 approximately (0.100 at 3.5 million, 0.102 at 6 million). By comparison, for tests without suction, at an incidence of 2.5° the increase in

Reynolds number from 3.5 million to 6 million increases the lift coefficient by 0.048.

The drag polars present a similar picture though they make a less consistent set, partly because of the difficulty of determining drag precisely from wake pitot traverses when the flow contains shock waves. Fig 9 shows the effect of full suction on the drag polar at a Reynolds number of 6 million. It is found that, at both Reynolds numbers, the effect of full suction is to reduce the drag coefficient at a given lift coefficient by between 0.03 and 0.04. Fig 10 shows the suction "off" polars at the two Reynolds numbers, the polar at the higher Reynolds number being the lower by between 0.015 and 0.02 in drag coefficient. As with lift coefficient, the effect of the suction is approximately twice that of the increase in Reynolds number.

4.3 Assessment of skin-friction formulae

The results from the 2D Tunnel provided a basis for assessing the skin-friction models used in BVGK. After many exploratory comparisons, it was decided that the most consistent data were the lift curves obtained, at both tunnel Reynolds numbers, with transition fixed at 5% chord on both upper and lower surfaces. Although there was a significant difference between the levels of the curves from BVGK and the tunnel,

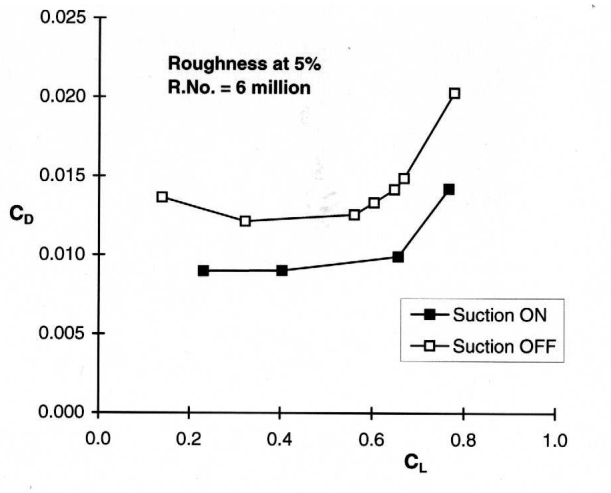

Figure 9. 2D aerofoil: effect of suction on drag polars at R = 6 million

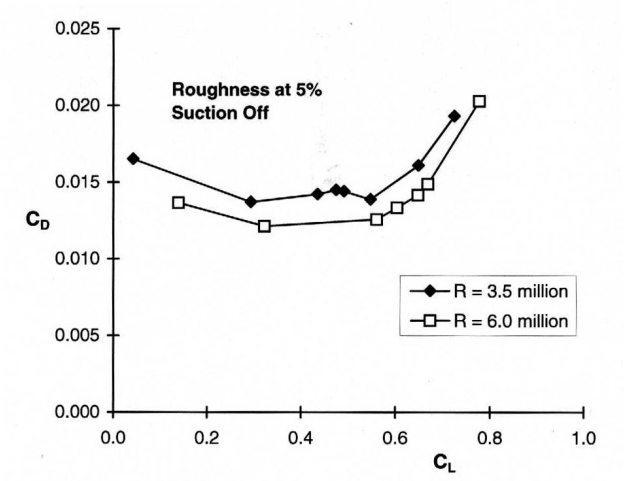

Figure 10. 2D aerofoil: effect of Reynolds number on drag polars with zero suction

attributable to the interference corrections applied to the tunnel data, it was argued that these corrections did not significantly affect the lift increments caused by the application of suction. These increments were therefore adopted as the yardstick against which the alternative friction models in BVGK were evaluated.

The assessment was made at a set Mach number of 0.735 and a lift coefficient of 0.6. Calculations were performed at both Reynolds numbers with zero suction and with the estimated experimental suction distributions, the latter being derived from the measured total flow through each panel. The procedure adopted to reduce the effect of experimental scatter was to fit least-squares straight lines to each set of lift versus incidence data from the tunnel and to do the same for BVGK calculations, for models A and C only, over similar ranges of lift coefficient. From the least squares fits, the values of α at a lift coefficient of 0.6 were determined and hence the reductions in α at this lift coefficient caused by the application of full suction were obtained. The results were as follows:

Method	Re million	Suction	α	Δα
2DT	3.5	OFF	3.011	
2DT	3.5	FULL	2.365	-0.655
2DT	6.0	OFF	2.668	
2DT	6.0	FULL	2.014	-0.654
BVGK	3.5	OFF	2.494	
BVGK	3.5	(A)	1.798	-0.696
BVGK	3.5	(C)	1.479	-1.015
BVGK	6.0	OFF	2.218	
BVGK	6.0	(A)	1.521	-0.697
BVGK	6. 0	(C)	1.201	-1.017

The striking feature of these results is that the increments are essentially the same at both Reynolds numbers in both the tunnel tests and in the BVGK calculations. This is taken as a powerful indication that the modelling of suction effects in BVGK is fundamentally sound. At the same time, the results show that both skin friction models are optimistic in predicting a greater effect than measured for a given level of suction. Model A overpredicts by about 5%, model C by 55%.

Following this comparison, it was decided to use model A, modified to correct the overprediction, in all further BVGK calculations. Because of the simplicity of the model, the correction was easily made by changing an empirical constant without changing the basic premise on which the model rested. The revised model was termed model A2. No further work directly to assess its accuracy or general applicability has been undertaken and the subject of the influence of suction on skin friction is still in need of a definitive experimental study. Nevertheless, its incorporation in BVGK produced a method which, in its overall comparison with the 2D Tunnel tests with suction, showed an accuracy comparable to that of the well established version of the code for aerofoils with solid surfaces.

5 Tests on a Swept-Wing Model

5.1 Model details

Fig 11 shows the swept wing semi-span model in the test section of the TWT. The wing semi-span was 52in. while the tunnel test section measures 9ft × 8ft. The model was tested only as a clean wing/fuselage combination. The fuselage was a veteran of previous project development testing but the wing was entirely new.

Figure 11. Semi-span model installed in TWT

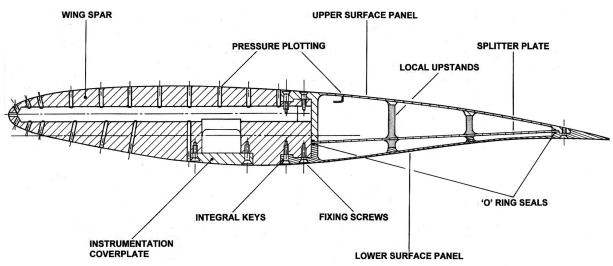

Figure 12. Semi-span model: typical wing cross section

Fig 12 shows a typical cross section through the wing. Two significant differences from the two-dimensional model were the use of a single suction panel on the upper surface and the position of the lower surface panel over the rear of the aerofoil rather than at mid chord. The results of the 2D tests, supported by modelling using BVGK and other tools, suggested a division in the suction flow between upper and lower surfaces in the ratio three to one.

The splitter plate in the suction passage divided the cross section area in that ratio and the original design of the flow passages in the wing root block, and the ducting leading to the suction plant, made provision for controlling and measuring the upper and lower surface suction rates independently. However, after rig tests to measure pressure drops along the suction ducting, this concept was abandoned. The passages at the wing root were re-designed so as to merge the two flows at the wing root and split them evenly between the two suction lines out of the tunnel.

On the basis of flow modelling, the target porosities for the upper and lower surfaces were set at 0.7% and 0.2% respectively. In the event, it proved difficult to achieve consistency of hole size in the laser drilling of the panels, which had been machined from solid and were not of perfectly uniform thickness. After manufacture, the distribution of porosity over both panels was measured by a suction probe and the planning of the wind tunnel tests was based on the achieved properties of the perforated surfaces rather than their nominal properties.

5.2 Simulation methodology

The methodology adopted was to aim to simulate a particular Reynolds number by a suitable combination of suction and transition trip location. The chosen simulation criterion was displacement thickness at the trailing edge, as predicted by the lag-entrainment method [8] modified to include suction with skin-friction model A2. The datum configuration, designated 36070, was targeted to simulate a factor of 10 increase in Reynolds number, 43 million as against the tunnel value of 4.3 million based on mean aerodynamic chord. Calculations were done for four spanwise control stations, the wing root, crank, 90% net span and the tip of the suction duct, and transition trip locations chosen to provide the target displacement thickness at the trailing edge under full suction conditions (ie all holes choked). The trips were installed as straight lines between the control stations. The trip for the baseline configuration was termed trip R20/a.

The achieved porosity on the lower surface panel was significantly greater than specified and so, for the datum configuration, part of the perforated area was sealed with gum arabic (and rubbed down to restore the original contour). The sealing was done from the trailing edge forwards such that, at each control station, the ratio of the calculated suction flow rates through the upper and lower panels was in the ratio 7:2 as originally intended. A position for the transition trip (trip R20/a) on the lower surface was chosen so that the predicted displacement thicknesses at the trailing edge matched the targeted values at 43 million Reynolds number on both upper and lower surfaces.

With this datum configuration of suction and transition trip R20/a, modelling indicated that Reynolds numbers lower than 43 million might be simulated by reducing suction rates. It was clear, however, that when this was done the suction holes would become unchoked and the spanwise distribution of suction would be changed significantly. Reducing suction would therefore provide only an approximate simulation of an intermediate Reynolds number. Even so, the test campaign included tests on the datum configuration with two reduced suction rates, aimed nominally at Reynolds number increases by factors of 5.65, corresponding to a Reynolds number of 24.4 million, and 4, to match the Reynolds number of 17 million for

which data were available for a corresponding full-span model tested in ETW.

A more complete simulation of an intermediate Reynolds number was explored by modelling and a second configuration, designated 36080, was devised, aimed at a factor of 5.65 increase in Reynolds number. This had the same trip on

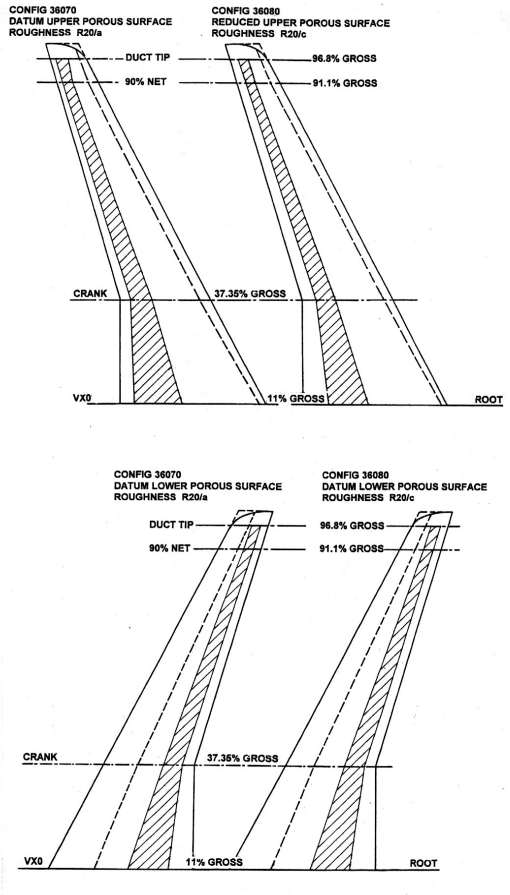

Figure 13. Wing plan showing porous area and transition trip for configurations 36070 and 36080

the upper surface as the datum configuration, but had the open area of the upper suction panel reduced by almost 40% using gum arabic. On the lower surface, the suction panel was retained unchanged from the datum but the transition trip was moved forward by approximately 5% of chord. This combination of surface trips was designated R20/c. The configuration also was tested with reduced suction, nominally to simulate a factor of 4 increase in Reynolds number.

The open suction areas and transition trip locations for these two configurations are shown in fig 13. Other combinations of suction and trip were tested, notably a configuration which replicated one of the trip geometries (designated BAeA) used in tests by BAe on a full-span model in ETW. At the end of the test campaign, the entire porous surface was sealed with gum arabic and rubbed down to provide a solid surface baseline. Tests with this sealed configuration and the BAeA trip provided a direct read across to the ETW tests.

5.3 Lift, drag and pitching moment

In all, nine different combinations of suction and trip configurations were tested, the most interesting ones being tested at five Mach numbers in the range 0.65 to 0.82. The data show a high degree of consistency and are well

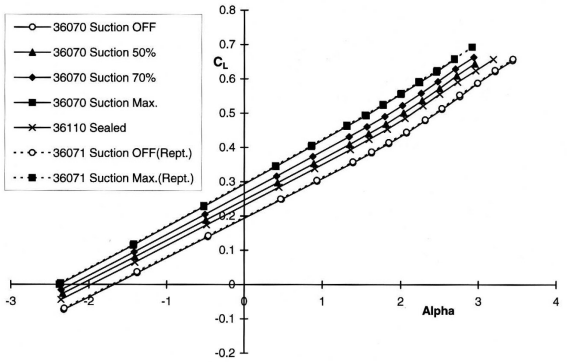

Figure 14. Semi-span model: variation of lift with incidence for datum suction area and R20/a trip, configurations 36070/071/110, M = 0.78

illustrated by the results for the datum suction configuration with trip R20/a, configuration 36070, at Mach 0.78, the cruise Mach number. Fig 14 shows the variation of lift coefficient with incidence for configuration 36070 and the repeat configuration, 36071. The five curves are for suction "full", suction "off", two intermediate suction settings and for the fully sealed model with the same trip, configuration 36110.

Corresponding curves of drag and pitching-moment coefficients against lift coefficient are

given in figs 15 and 16. The coefficient C_{D0} in fig 15 is the total drag coefficient C_D as determined from the balance, less the momentum drag coefficient of the suction flow $2m_s/\rho_\infty U_\infty S$ and the nominal vortex drag coefficient $C_L^2/\pi A$. In conventional wind tunnel tests without suction, C_{D0} is commonly adopted as an approximate measure of the combined viscous and wave drag of the model.

The graphs show similar effects of suction on all configurations. Increasing suction increased lift at a given incidence and reduced drag and increased nose-down pitching moment at a given lift.

As is clear from these figures, the re-circulation which arises when testing with suction "off" had the opposite effect to applying suction, the effect being much greater than found in the 2D tests. In the 2D tests, each suction panel was backed by a sealed cavity and the relatively small re-circulation which occurred with suction "off" was an inflow and balancing outflow through the panel, driven by the external pressure variation along the panel. The effect was analysed and BVGK was adapted to include a model of it, which was used in the BVGK calculations for the zero suction case. In the case of the 3D model, the upper and lower suction ducts, though divided by a splitter plate, were connected at the wing root. This enabled flow to pass from the lower to the upper duct

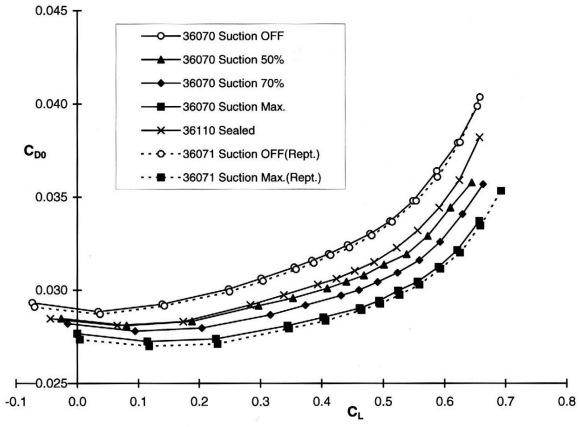

Figure 15. Semi-span model: variation of drag with lift for datum suction area and R20/a trip, configurations 36070/071/110, M = 0.78

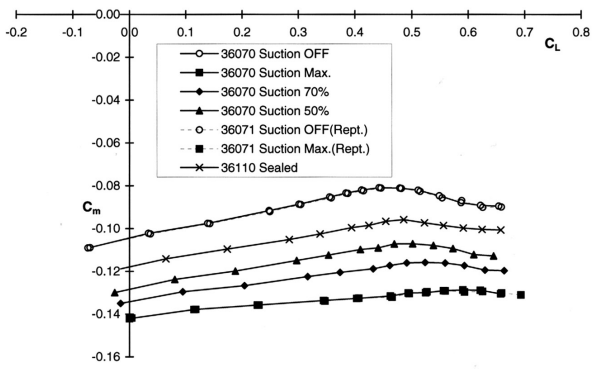

Figure 16. Semi-span model: variation of pitching moment with lift for datum suction area and R20/a trip, configurations 36070/071/110, M = 0.78

and analysis of the measured pressures showed that, with suction "off", there was an inflow over the entire lower suction panel and a corresponding net outflow through the upper panel. The rate of outflow though the upper panel was comparable to the inflow through the panel at intermediate suction rates.

Close examination of the figures shows that the shapes of the drag and pitching moment polars for the sealed wing differ slightly from those of the adjacent reduced suction cases. This is attributed to the fact that the reduction in suction flow, and the change in its spanwise distribution, was much greater on the upper surface than the lower. In some cases, this resulted in local outflow from the forward part of the upper surface panel over parts of the span.

5.4 Effect of varying suction rate

The variation of force and moment coefficients with suction rate was explored by plotting incremental values of the coefficients against linear combinations of the upper and lower surface suction coefficients. The datum for the increments was taken as the fully sealed wing with the same configuration of transition trip. The exploration was confined to the design Mach number, 0.78, and to three parameters: the increment in lift coefficient at an incidence of 2°; the increment in the lift-adjusted drag coefficient C_{D0} at a lift coefficient of 0.4; and the "critical" pitching moment coefficient C_{mc} at

the break in the pitching moment/lift polar. The derivation of C_{mc}, as the point of intersection of two straight lines fitted through the sections of the polar below and above the critical condition, is shown in fig 17.

The results for all configurations that were tested with reduced as well as full suction rates were pooled. The intermediate suction rates achieved by reducing the ejector drive pressure did not reduce suction through the upper and lower surfaces in equal proportions. For configuration 36070, for example, upper surface

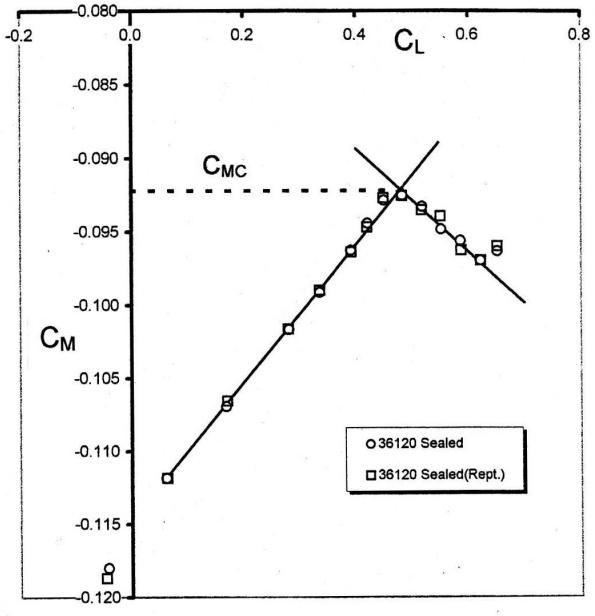

Figure 17. Pitching moment polar showing derivation of C_{MC}

suction varied by a factor of 4 while lower surface suction varied by less than 25%. Also, it had been found in the experiment on the 2-D aerofoil that upper surface suction was about 8 times as powerful as lower surface suction in its effect on lift at a given incidence.

With these two complicating effects at work, plotting force and moment coefficients against total suction rate was not expected to present a clear picture. As an alternative, for each coefficient, the method of least squares was used to determine the linear combination of upper and lower surface suction which gave the best straight line through the origin, in the form $\Delta C_x = A(C_{qu} + kC_{ql})$, for all the data in the pool. The suction coefficients C_{qu} and C_{ql} are respectively the upper and lower surface values for the total suction coefficient C_{qt} for each surface, defined as

$$C_{qt} = \int_s \frac{\rho_w v_w}{\rho_\infty U_\infty} \frac{dx}{c} \quad .$$

For the pooled data, the value of the weighting parameter k determined in this way was 0.058 for lift, 0.067 for drag and 0.085 for pitching moment, giving an average value of 0.07. Because the variation of C_{ql} was an order of magnitude less than the variation of C_{qu}, there was no significant loss of accuracy in adopting this average value of k as the lower surface suction weighting factor for all three force and moment coefficients. In overall comparisons, the weighted suction coefficient ($C_{qu} + 0.07C_{ql}$) was found to be an adequate basis for relating results for all configurations tested with reduced as well as full suction.

5.5 Assessment of simulation

One obvious test of the experimental results is to compare them with predictions by a three-dimensional viscous CFD method. Comparisons with codes available at the time proved unfruitful, however, partly because of limitations in their post-processing capabilities. Then, at a late stage in the assessment of the experimental results from the TWT, BAe made available data obtained on a corresponding full span model tested in the European Transonic Windtunnel (ETW). These results, for a model to the same aerodynamic design as R20, covered a range of Reynolds number from 3.2 to 17 million. The results were complicated by the use of different standards of transition trip over different parts of the Reynolds number range, by the effects of aeroelastic distortion, and by the fact that some of the variation of Reynolds number was achieved by varying pressure at constant temperature and some by varying temperature at constant pressure. They were made available in an uncorrected state. Despite

these complications, the data do appear to provide a credible basis for assessing the quality of simulation achieved in the TWT tests on R20.

It was found that comparison between the lift curves in the two facilities was not fruitful because of aeroelastic distortion of the wing over the wide range of stagnation pressure in the ETW tests. It proved possible, however, to use both the pitching moment and drag data to create a read-across between the two sets of tests.

For pitching moment, the parameter chosen was the critical pitching moment coefficient C_{mc} at the break in the pitching moment/lift curve at Mach 0.78 (see figs 16 and 17) which could be determined consistently and unambiguously from both sets of data. In the R20 tests, this feature occurred at the same incidence as a kink in the trailing pressure on the outer wing and was suction dependent. In the ETW tests it was Reynolds number dependent. The values of C_{mc} obtained for the ETW tests are shown in their raw form, plotted against the log to base 10 of Reynolds number based on mean aerodynamic chord, in fig 18.

As indicated on the figure, the method of varying Reynolds number was to increase tunnel pressure at constant temperature over the upper

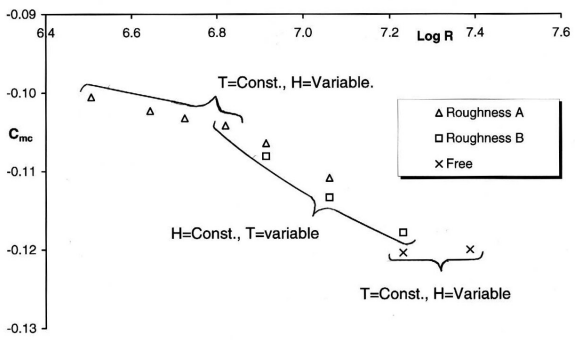

Figure 18. Variation of C_{MC} with Reynolds number for full-span model in ETW

and lower Reynolds number ranges and to decrease temperature at constant pressure over the middle range. Consequently, the results in the upper and lower ranges were subject to much stronger aeroelastic effects than in the middle range. A further complication was the three different transition locations (two trips and transition free).

The approach taken to correcting for these factors was to assume that, in the absence of tunnel pressure variation, the data for a particular transition trip would vary linearly with the log of Reynolds number and that the slope of the line would be independent of trip location. The results of varying Reynolds number at constant pressure would then be a series of parallel straight lines, one for each trip position. By a least squares fitting process, the slope of the constant pressure line was determined from the mid-range data, which had been obtained by varying temperature at a constant stagnation pressure of 2.6 atm. A straight line was also fitted to the low-range data, which had been obtained by varying stagnation pressure at constant temperature, and the difference in slopes between the two lines was taken to define the influence of aeroelasticity on C_{mc}. The results plotted in fig 18 were then adjusted from the stagnation pressure of the test to a constant stagnation pressure of 3 atm by applying the correction so derived. (The ETW model was designed so that, at a tunnel pressure of 3 atm and at cruise lift coefficient, the wing shape would match the aircraft in 1g flight).

The ETW results, corrected in this way, are plotted in fig 19 and are seen to be well fitted by three parallel straight lines, including the high Reynolds number, free transition data which played no part in deriving the pressure correction. What this figure is argued to show is the variation with Reynolds number of C_{mc} for a wing of essentially constant shape.

A direct read-across from the ETW tests to R20 is possible because one R20 configuration was tested with sealed suction surfaces and with a transition trip to the same specification as Trip A in the ETW tests. The value of C_{mc} for this

configuration, 36120, was 0.00475 above the line fitted through the ETW data for Trip A in fig 19. This difference, thought to be attributable mostly to aeroelastic effects, was subtracted from the R20 data for the two main configurations to align them with ETW.

In fig 20 the R20 results, so corrected, are plotted onto the straight lines fitted to the ETW results in fig 19. The data shown are for configuration 36120, which fits onto the Trip A line at a Reynolds number of 4.3 million, and for configurations 36070 and 36080 at full and intermediate suction rates, plotted to lie on the ETW transition free line. The Reynolds numbers at which the latter points are plotted are taken as the Reynolds numbers simulated in the test. The maximum Reynolds numbers of

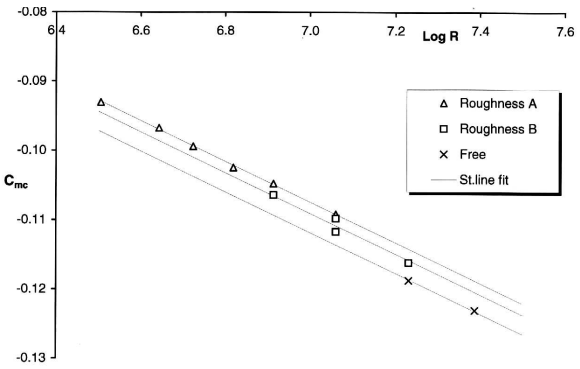

Figure 19. Projected variation with Reynolds number of C_{MC} at constant 3 bar for full span model in ETW

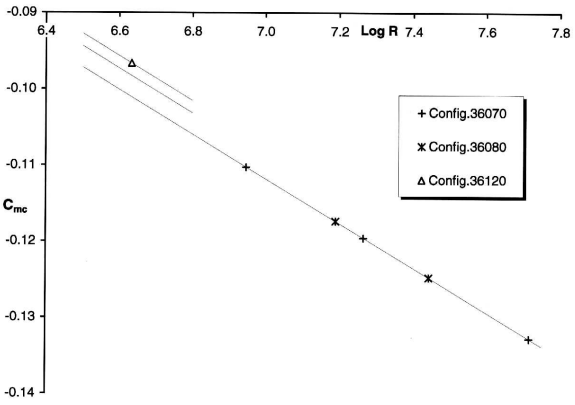

Figure 20. Correlation of R20 and ETW pitching moment data

the plotted points are 51 million for configuration 36070 and 28 million for 36080.

Comparison between R20 and ETW drag measurements is complicated by the fact that the available data from ETW are for a complete wing-body model with fin and flap-track fairings and are uncorrected for sting interference, while the R20 results are for a clean wing on a half-model. A more serious complication is the fact that Reynolds number variation in ETW affects the drag of the entire model while suction affects only the wing drag on R20. Despite these complications, it has been possible to formulate a read-across from R20 to ETW by comparing the variation of the estimated wing-alone drag of R20 with that of the drag of the complete model in ETW.

The ETW drag measurements come from the same data points as the pitching-moment results in figs 18 and 19, with the Reynolds number range covered by a combination of pressure and temperature variation and with transition free or fixed by one of two alternative trips. The data available to ARA were uncorrected measurements of the lift-adjusted drag coefficient C_{D0} at a lift coefficient of 0.4. When plotted against Reynolds number, these data fell on three curves, one for each standard of transition fixing. Unlike the pitching-moment data, however, they did not show any clear evidence of being influenced by aeroelastic distortion and no attempt has been made to identify and correct for aeroelastic effects.

There was some Reynolds number overlap for the different trip configurations which enabled drag increments to be estimated for each trip and subtracted to bring the data to a common baseline. The resulting data, plotted as the log of drag coefficient against the log of Reynolds number fell, on a smooth curve, fig 21, which was taken to be the variation of drag with Reynolds number for a wing with free transition at the a lift coefficient of 0.4. For clarity, coincident points have been shifted along the

slope of the curve. The fit to the data is reasonably good, the greatest scatter being approximately one drag count. The reference data point is at a Reynolds number of 4.4 million, close to the 4.3 million of the R20 tests.

To put the R20 data in a comparable form, it was necessary to identify the drag of the wing alone at a Reynolds number of 4.3 million. By a series of careful cross references, making use of data from both full-span and half-model tests in the TWT, it was possible to derive values for the fuselage drag of the R20 half-model at a C_L of 0.4 and, hence, of the wing-alone drag of configurations 36070 and 36080 and the corresponding sealed-wing configurations 36110 and 36100. The wing drag for the two sealed configurations, adjusted for trip drag, was identical and was taken as the reference for the drag reduction achieved by suction.

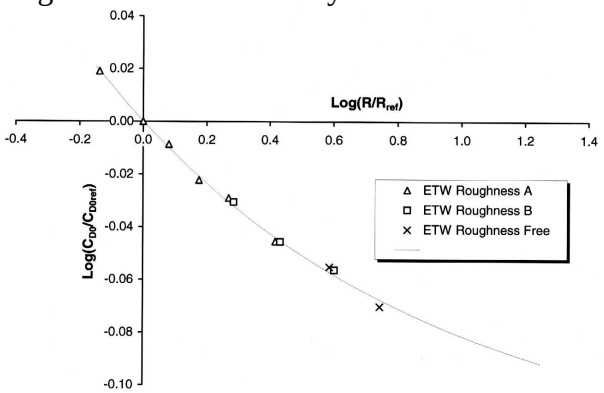

Figure 21. Correlation of ETW drag results

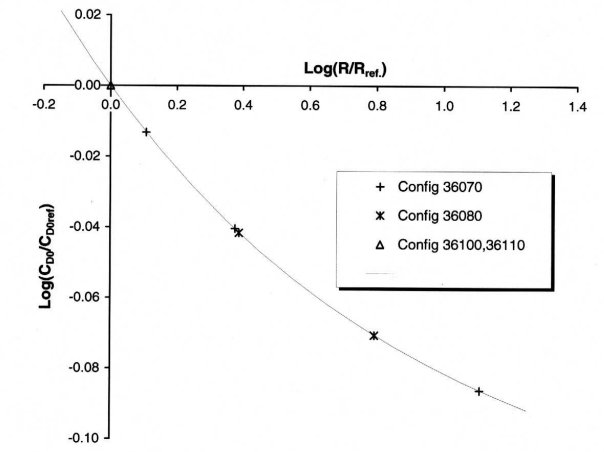

Figure 22. Correlation of R20 and ETW drag data

In fig 22 the experimental results from R20, in the form $\log(C_{D0w}/C_{D0wref})$, are plotted on the curve fitted through the ETW data in fig 21. As in fig 20, **t**he Reynolds numbers at which the R20 points are plotted are taken as the Reynolds numbers simulated in the test. The maximum Reynolds numbers of the plotted results are 55 million for configuration 36070 and 27 million for configuration 36080

The results of the read-across to ETW shown in figs 20 and 22 are summarised in the table below, which also shows the target Reynolds numbers for the two configurations. The targets at intermediate suction rates have been derived by interpolation in the series of boundary layer calculations undertaken during the final planning of the TWT test programme. The suction coefficient used in the interpolation was the same as noted in section 5.4 above, $C_{qu} + 0.07C_{ql}$.

Config.	$C_{qu} + 0.07C_{ql}$	Simulated Re (millions)		
		Target	From C_{mc}	From C_{Dow}
36070	1.222	43.0	50.8	55.1
	0.649	17.9	18.4	10.3
	0.317	10.7	8.9	5.5
36080	0.902	24.4	27.7	26.7
	0.598	16.5	15.5	10.3

Summary of Reynolds numbers simulated on semi-span model

The picture presented by this table is very encouraging. It strongly suggests that the basic premise underlying the R20 project is sound. Indeed, it indicates that the primary goal of the programme, of demonstrating the successful application of the suction technique on a realistic three-dimensional model in the TWT, has been achieved. Considered together with the results of the 2D aerofoil tests and the theoretical methods developed for flows with suction, it gives reassurance that the technique can be developed into a viable and flexible method of simulating full-scale Reynolds numbers on half models in the ARA TWT.

6 Conclusions

The R20 programme set out to demonstrate the feasibility of simulating the aerodynamics of a transport aircraft wing at full-scale Reynolds numbers by applying boundary layer suction to a semi-span model tested in the ARA Transonic Wind Tunnel. The main achievements of and conclusions from the parts of the programme described in this paper are as followed:

(1) CFD codes have been developed for aerofoil design and boundary layer prediction including the effects of boundary-layer suction. These codes provide a credible basis for the design of future configurations aimed at simulating high Reynolds number by suction.

(2) Preliminary experiments on an aerofoil in the 2D Tunnel played a key role in demonstration of the concept and in validation of the CFD codes.

(3) Advances in model design and manufacture were made and many lessons learned.

(4) A methodology for simulating high Reynolds numbers by a combination of aft transition fixing and boundary-layer suction in a half-model tested in the ARA Transonic Wind Tunnel was developed and successfully demonstrated. Comparisons with test results from ETW imply that the highest mean-chord Reynolds number simulated in the R20 half-model tests was in excess of 50 million.

(5) Further work is needed to translate the suction technique from a demonstrated concept into a fully developed tool for wind tunnel testing. The achievement of high Reynolds number aerodynamics without a difficult test environment, as a supplement to ETW testing and an insurance against possible future ETW outages, must be a goal worth pursuing.

References

[1] Bocci, A.J. Aerofoil design for full-scale Reynolds number. ARA Memo 211, 1979.

[2] Lanchester, F.W. *Aerodynamics.* Constable & Co., London, 1907.

[3] Loving, D.L. Wind tunnel-flight correlation of shock-induced separated flow, NASA TN D-3580, Sept 1966.

[4] Green, J.E. A discussion of viscous-inviscid interaction at transonic speeds. RAE TR 72050, May 1972.

[5] Green, J.E. Second Goldstein Lecture. Modern developments in fluid dynamics an addendum. *The Aeronautical Journal*, Vol.96, No. 953, pp 69 - 86, March 1992.

[6] Boundary layer simulation and control in wind tunnels. AGARD-AR-224, Report of AGARD WG09, Ed. M.L.Laster.

[7] Ashill, P.R., Wood, R.F., Weeks, D.J. An improved, semi-inverse, version of the viscous Garabedian and Korn method (VGK), RAE TR 87002, 1987.

[8] Green, J.E., Weeks, D.J. and Brooman, J.W.F. Prediction of turbulent boundary layers and wakes in compressible flow by a lag-entrainment method. ARC R&M 3791, 1973.